THE EFFECTS OF TRANSFORMATION METHODS IN IMAGE WATERMARKING

Prayoth Kumsawat[1], Kitti Attakitmongcol[1] and Arthit Srikaew[2]

[1]Signal and Image Processing Research Group, School of Electrical Engineering
Institute of Engineering, Suranaree University of Technology
111 University Avenue, Muang District, Nakhon Ratchasima, Thailand.30000
{prayoth, kitti}@ccs.sut.ac.th
[2]Intelligent System Research Group, School of Electrical Engineering
Institute of Engineering, Suranaree University of Technology
111 University Avenue, Muang District, Nakhon Ratchasima, Thailand.30000
ra@ccs.sut.ac.th

ABSTRACT

Image watermarking provides copyright protection and becomes very crucial for ownership verification of digital images. In this paper, we investigate the effects of different types of transformations in image watermarking algorithm including discrete cosine transform, discrete wavelet transform, and discrete multiwavelet transform. We also provide a brief overview of the multiwavelet transform since it is relatively new as compared to the other transforms. The efficiencies of these transforms are discussed by evaluating watermarked image quality and robustness of the watermark. Experimental results show that the multiwavelet transform method is superior to other two methods in term of image quality.

1. INTRODUCTION

Due to the rapid and extensive growth of the internet, intellectual property protection is a pressing concern for owners who are exhibiting digital representations of the photographs or original artworks. Digital watermarking is one of the most popular approaches considered as a tool for providing the copyright protection of digital images. This technique is based on embedding a digital signature into the digital images. Ideally, there should be no perceptible difference between the watermarked and original images, and the watermark should be easily extractable, reliable and robust against image compression or common image processing. In general, we can classify digital watermarking into two classes depending on the domain of watermark to be embedded: the spatial domain watermarking and the transform domain watermarking.

Currently, watermarking techniques based on transform domain are more popular than those based on spatial domain since they provide higher image quality and much more robust watermark. Cox *et al.* [1] proposed a watermarking technique by embedding the watermark in the discrete cosine transform (DCT) domain of an image using the concept of spread

spectrum communication. Xia *et al.* [2] introduced a new multiresolution watermarking method based on the discrete wavelet transform (DWT). The watermark is embedded to the large wavelet coefficients at high and middle frequency bands of the image's DWT. Song *et al.* [3] gave the comparison of difference watermarking techniques by focus on the evaluation of robustness and visual quality property. S. H. Yang [4] has concentrated on the evaluation of biorthogonal wavelets using spread-spectrum watermarking framework.

In this paper, we investigate the effects of three different transformation methods including discrete cosine transform, discrete wavelet transform and discrete multiwavelet transform. All transform methods are performed on the same platform using the spread spectrum image watermarking technique. In the spread spectrum watermarking, the watermark insertion is like transmitting a spread spectrum signal (the watermark) through a noisy environment (the original image). We then compare the experimental results of these three transformation methods.

2. TRANSFORMATION METHODS

Discrete cosine transform (DCT) is commonly used in MPEG and JPEG as an orthogonal transform. In DCT domain, the energy concentrates in the low frequency regions around the upper-left corner. Figures 1(a) and 1(b) show the original Lena image and its transformed coefficients using DCT.

Figure 1. (a) Original "Lena" image, (b) transform coefficients of "Lena" image obtained by DCT.

Discrete wavelet transform (DWT) can decompose the image into different frequency bands and still retain the spatial information. In wavelet watermarking techniques, since DWT of an image gives multiresolution representation, this allows the

independent processing of the resulting components and the trade-off between robustness and invisibility can be decently made.

Discrete multiwavelet transform (DMT) is relatively new type of signal transform that is commonly used in image compression. The main motivation of using multiwavelet is that it is possible to construct multiwavelets that simultaneously possess desirable properties such as orthogonality, symmetry and compact support with a given approximation order. These properties are not possible in any real-valued scalar wavelet (wavelet based on one scaling function). Next we give a brief overview of the multiwavelet transform.

Let Φ denote a compactly supported orthogonal scaling vector $\Phi = (\phi^1, \phi^2, ..., \phi^r)^T$ where r is the number of scalar scaling functions. Then $\Phi(t)$ is satisfy a two-scale dilation equation of the form

$$\Phi(t) = \sqrt{2} \sum_n h(n)\Phi(2t - n) \qquad (1)$$

for some finite sequence h of $r \times r$ matrices. Furthermore, the integer shifts of the components of Φ form an orthonormal system, that is

$$< \phi^l(\cdot - n), \phi^{l'}(\cdot - n') > = \delta_{l,l'}\delta_{n,n'}.$$

Let V_0 denote the closed span of $\{\phi^l(\cdot - n) \mid n \in Z, l = 1, 2, ..., r\}$ and define $V_j = \{f(\frac{\cdot}{2^j}) \mid f \in V_0\}$. Then $(V_j)_{j \in Z}$ is a multiresolution analysis of $L^2(R)$ [5]. Note that we choose the decreasing convention $V_{j+1} \subset V_j$.

Let W_j denote the orthogonal complement of V_j in V_{j-1} Then there exists an orthogonal multiwavelet $\Psi = (\psi^1, \psi^2, ..., \psi^r)^T$ such that $\{\psi^l(\cdot - n) \mid l = 1, 2, ..., r$ and $n \in Z\}$ form an orthonormal basis of W_0. Since $W_0 \subset V_{-1}$, there exists a sequence g of $r \times r$ matrices such that

$$\Psi(t) = \sqrt{2} \sum_n g(n)\Phi(2t - n). \qquad (2)$$

Let $f \in V_0$, then f can be written as a linear combination of the basis in V_0.

$$f(t) = \sum_n c_0(k)^T \Phi(t - k) \qquad (3)$$

for some sequence $c_0 \in l_2(Z)^r$. Since $V_0 = V_1 \oplus W_1$, f can also be expressed as

$$f(t) = \frac{1}{\sqrt{2}} \sum_{k \in Z} c_1(k)^T \Phi(\frac{t}{2} - k)$$
$$+ \frac{1}{\sqrt{2}} \sum_{k \in Z} d_1(k)^T \psi(\frac{t}{2} - k). \qquad (4)$$

The coefficients c_1 and d_1 are related to c_0 via the following decomposition and reconstruction algorithm:

$$c_1(k) = \sum_n h(n)c_0(2k + n) \qquad (5)$$

$$d_1(k) = \sum_n g(n)c_0(2k + n) \qquad (6)$$

$$c_0(k) = \sum_n h(k - 2n)^T c_1(n)$$
$$+ \sum_n g(k - 2n)^T d_1(n). \qquad (7)$$

Unlike scalar wavelet, even though the multiwavelet is designed to have approximation order p, the filter bank associated with the multiwavelet basis does not inherit this property. Furthermore, since the multiwavelets have more than one scaling function, the dilation equation becomes a dilation with matrix coefficients. Thus, in applications, one must associate a given discrete signal into a sequence of length $-r$ vectors (where r is the number of scaling functions) without losing some certain properties of the underlying multiwavelet. Such a process is referred to as prefiltering or multiwavelet initialization. The block diagram of a multiwavelet with prefilter $Q(z)$ and postfilter $P(z)$ is show in figure 2. $H(z)$ and $Q(z)$ are the z transform of $h(n)$ and $g(n)$, respectively. The sequence x is a vector-valued sequence obtained by the following operator. Define the operator $D_r : R^Z \to (R^r)^Z$ which partitions a scalar sequence into a sequence grouped in vectors of length r as follows. Given a scalar sequence $x(n)$, $n \in Z$ then $x = D_r(x)$ is given by

$$x = D_r(x) = (\downarrow r) \begin{pmatrix} x(n) \\ x(n+1) \\ \vdots \\ x(n+r-1) \end{pmatrix}_{n \in Z}$$
$$= \begin{pmatrix} x(rn) \\ x(rn+1) \\ \vdots \\ x(rn+r-1) \end{pmatrix}_{n \in Z} \qquad (8)$$
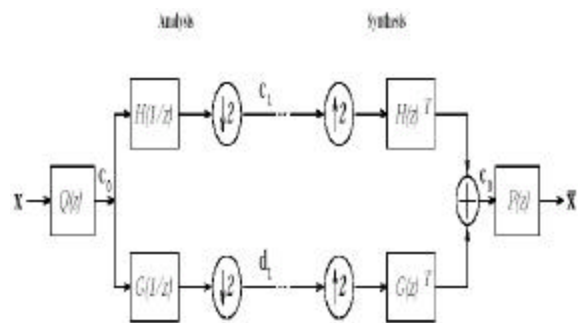

Figure 2. Multiwavelet filter bank.

Similar to the traditional scalar wavelet transform, the two-dimensional multiwavelet transform can be achieved by applying the one-dimensional transform on the rows by treating each row as a one-dimensional signal and afterward on columns. However, for the applications using multiwavelets, prefiltering process must be applied to

each row and each column to initiate the vector sequence $\mathbf{c_0}$ to the filter bank. Figures 3(a) and 3(b) show the image subbands of three-level wavelet decomposition using Daubechies-8 filter and three-level multiwavelet decomposition using the DGHM multiwavelet, respectively.
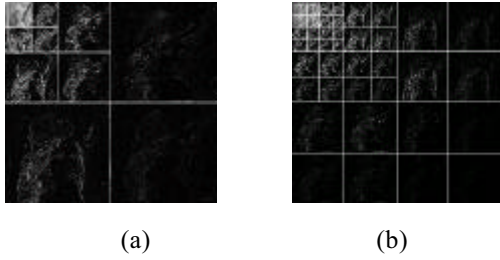

<center>(a)   (b)</center>

Figure 3. Image subbands of "Lena" image obtained by (a) three-level wavelet decomposition using D8 filters (b) three-level multiwavelet decomposition using the DGHM multiwavelet (with prefiltering).

3. SPREAD SPECTRUM WATERMARKING

Spread spectrum communication is a popular analogy for watermarking. The well-known spread spectrum watermarking technique is proposed by Cox *et al.*[1]. For this technique, the embedding procedure is like transmitting a spread spectrum signal (the watermark) thought a noisy environment (the original image). Watermark extraction is equivalent to the detection of the spread spectrum signal from an interference environment. The watermarking to be embedded is a sequence of 1,000 random numbers, having a Gaussian distribution $N(0,1)$. The watermark sequence is embedded in the 1,000 largest coefficients excluding the DC coefficients of DCT domain by the following equation:

$$V_i^{'} = V_i + \alpha V_i X_i \qquad (9)$$

, where V_i is the selected DCT coefficients, X_i is the watermark and α is the embedding strength. The watermarked image is obtained by the inverse DCT of $V_i^{'}$.

The detection process is the inverse procedure of the watermark insertion process. It is composes of transformation of the original image and watermarked image, and watermark extraction process. After extracting the watermark, similarity measurement between the original watermark and the extracted watermark is taken as a measurement of presence of the watermark. A similarity between X and X^* is defined in [1] as:

$$sim(X, X^*) = \frac{X \cdot X^*}{\sqrt{X^* \cdot X^*}} \qquad (10)$$

, where X is the original watermark and X^* is the extracted watermark. To decide whether the suspected image is a watermarked version of the original image, the tested result is compared to a fixed threshold $\delta\,(\delta = 6)$. If the similarity is greater

than the fixed threshold, the watermark has been detected.

4. EXPERIMENTAL RESULTS AND DISCUSSIONS

In this section, some experimental results are demonstrated to show the effects of the three transformations on the spread spectrum watermarking technique. All of the original images are gray-scaled standard image of size 512×512 pixels. To study the effects of transformation methods, we perform the same watermark insertion and watermark detection based on [1] with various transformation methods. For the cases of using DWT and DMT, we decompose an original image into 3 levels and the watermark is embedded to the 1,000 largest coefficients of all subbands, except for approximation subband. The embedding strength is 0.1 as in [1]. The performance of each transform-based watermarking scheme is measured by image quality and robustness of the watermark.

To measure the image quality of the watermarked image, we use the peak signal to noise ratio (PSNR) and mean structural similarity (MSSIM) [6]. The experimental results of image quality measured by PSNR and MSSIM are shown in figures 4 (a) and 4(b), respectively. The PSNR of the watermarked image with various embedding strengths is shown in figure 4 (c). From figure 4, the results clearly show that the method using DMT yields the best image quality. To verify the detecting uniqueness, we send the extracted watermark together with other 1,000 random watermarks to the correlation detector. The 500th watermark is the extracted watermark. From figure 5(a), we can see that the detector response of the real watermark is very high while other responses are very low.

To verify the robustness of the watermark under JPEG and JPEG2000 compression, we compressed watermarked image with Q factors varying from 10% to 100%. The similarities of the original and extracted watermarks are shown in figure 5(b) and 5(c) for JPEG and JPEG2000, respectively. We can see that the algorithm using DCT gives the most robust watermark.

To evaluate the robustness of the watermark under common image processing, we apply different types of attacks including 3×3 lowpass filtering and 3×3 Wiener filtering. In addition, we attack the watermarked image by adding Gaussian noise with variance of 500. Figures 6(a)-6(c) show the similarities of watermarks when the watermarked image is attacked by common image processing. From Figures 6(a)-6(c), we can also see that the method using DCT yields the most robust watermark under those attacks.

5. CONCLUSIONS

We have studied the effects of transformations including the discrete cosine, discrete wavelet and discrete multiwavelet transforms in the spread

spectrum watermarking algorithm. Due to the multiresolution representation obtained from using DWT and DMT, the algorithms using both transforms yield better image quality than the one using DCT. However, the algorithm using DCT gives the most robust watermark under compression and common image processing that were included in this study.

This is likely due to the fact that for the watermarking in the DCT domain, watermark spreads over a set of visually important frequency components. Further research can be focused on the development of robust watermarking method using the multiwavelet transform.
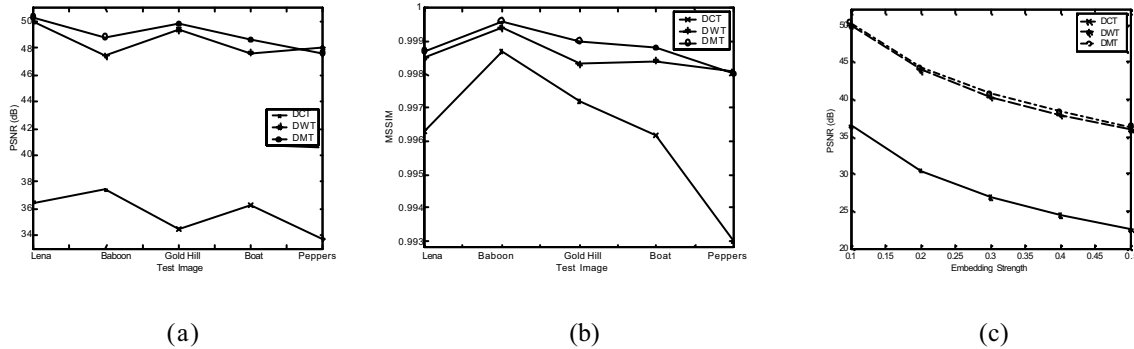
(a)   (b)   (c)

Figure 4. (a) PSNR of watermarked images using 5 test images (Lena, Baboon, Gold Hill, Boat, and Peppers) (b) MSSIM of watermarked image using 5 test images (c) PSNR of "Lena" watermarked image with different watermark strengths.
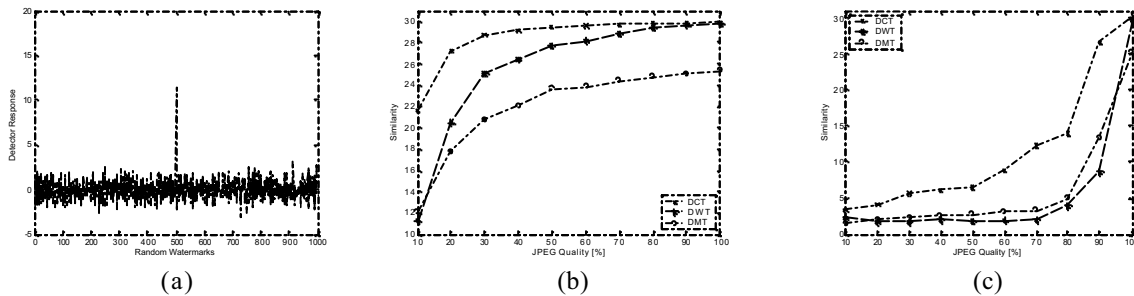
(a)   (b)   (c)

Figure 5. (a) Detector response of 1,000 watermarks including extracted watermark of Lena image using DWT under 10 % JPEG quality. (b) and (c) Similarities of watermarks under JPEG and JPEG2000 compressions, respectively.
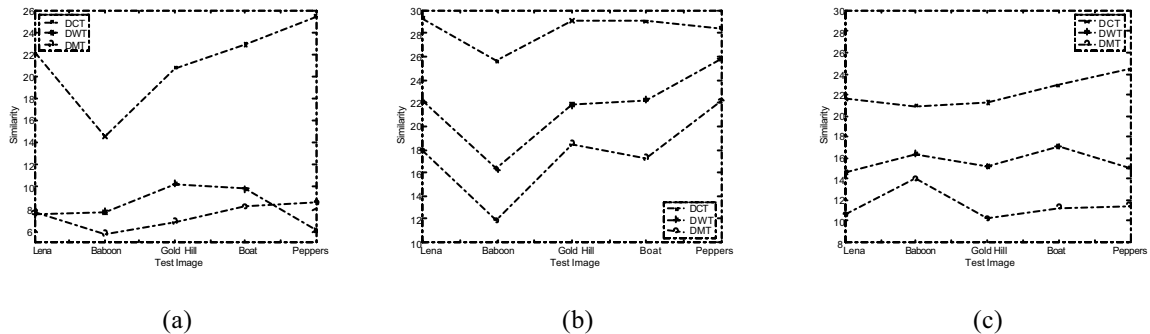
(a)   (b)   (c)

Figure 6. Similarities of watermarks under different types of attacks of 5 test images: (a) Lowpass filtering , (b) Wiener filtering , and (c) adding Gaussian noise.

7. REFERENCES

[1] I. J. Cox, J. Kilian, F. T. Leighton, and T. Shamoon, "Secure Spread Spectrum Watermarking for Multimedia," *IEEE Trans. on Image Processing,* vol. 6, pp. 1673-1687, Jan. 1997.

[2] X. -G. Xia, C. Boncelet, and G. Arce., "A Multiresolution Watermark for Digital Images," In *Proc. IEEE ICIP*, vol. 1, pp. 26-29, Oct. 1997.

[3] Y. J. Song and T. N. Tan, "Comparison of Four Difference Digital Watermarking Techniques," In *Proc. WCCC-ICSP* , vol. 2, pp. 946-950, Aug. 2000.

[4] S. H. Yang, "Wavelet Filter Evaluation for Image Watermarking," In *Proc. IEEE ICASSP*, vol. 3, pp. 525-528, Apr. 2003.

[5] K. Attakitmongcol, D. P. Hardin and D. M. Wilkes, "Multiwavelet Prefilters II: Optimal Orthogonal Prefilters," *IEEE Trans. on Image Processing,* vol. 10, pp. 1476–1487, Oct. 2001.

[6] Z. Wang, A. C. Bovik, H. R. Sheikh and E. P. Simoncelli, "Image Quality Assessment: From Error Measurement to Structural Similarity," *IEEE Trans. on Image Processing,* vol. 13, pp. 600-612, Apr. 2004.